Coherent Heavy Quasiparticles in a $CePt_5$ Surface Alloy

M. Klein,[1] A. Nuber,[1] H. Schwab,[1] C. Albers,[1] N. Tobita,[2] M. Higashiguchi,[2] J. Jiang,[2] S. Fukuda,[2] K. Tanaka,[2] K. Shimada,[3] M. Mulazzi,[1] F. F. Assaad,[4] and F. Reinert[1,5,*]

[1]*Universität Würzburg, Experimentelle Physik VII & Röntgen Research Center for Complex Materials RCCM, Am Hubland, D-97074 Würzburg, Germany*

[2]*Graduate School of Science, Hiroshima University, Higashi-Hiroshima 739-8526, Japan*

[3]*Hiroshima Synchrotron Radiation Center, Hiroshima University, Higashi-Hiroshima 739-0046, Japan*

[4]*Universität Würzburg, Institut für Theoretische Physik und Astrophysik, Am Hubland, D-97074 Würzburg, Germany*

[5]*Karlsruhe Institute of Technology KIT, Gemeinschaftslabor für Nanoanalytik, D-76021 Karlsruhe, Germany*

(Received 21 December 2010; revised manuscript received 1 April 2011; published 6 May 2011)

We report on the results of a high-resolution angle-resolved photoemission study on the ordered surface alloy $CePt_5$. The temperature dependence of the spectra show the formation of the coherent low-energy heavy-fermion band near the Fermi level. These experimental data are supported by a multiband model calculation in the framework of the dynamical mean-field theory.

DOI: 10.1103/PhysRevLett.106.186407 PACS numbers: 71.27.+a, 71.20.Eh, 75.30.Mb, 79.60.−i

The physics of f electrons continues to fascinate since the interplay between fundamental interactions gives rise to complex phase diagrams and exotic states of matter [1]. In Kondo systems, the two main energy terms determining the microscopical behavior are the hybridization between localized f states and conduction electrons and the large Coulomb repulsion between f electrons at the same lattice site. At temperatures above the coherence temperature T^* these interactions are purely local and can be explained successfully by the single-impurity Anderson model (SIAM) [2–5]. A very powerful tool which allows the study of these local interactions experimentally is photoemission spectroscopy as it directly probes the spectral function of the system. In the past the combination of photoemission spectroscopy (PES) and SIAM leads to a deeper understanding of Kondo systems spectral features like the Kondo resonance (KR) with additional spin-orbit and crystal-field excitations, including their temperature dependence [6,7]. Nevertheless, at temperatures $T \ll T^*$ the localized heavy quasiparticles begin to interact with each other and finally form coherent heavy-fermion bands whose properties cannot be explained by the SIAM any longer [2,8]. Up to now experimental limitations prevented a closer investigation of this coherent heavy-fermion state by photoemission. In order to observe coherence effects one usually needs temperatures well below the Kondo temperature T_K of the system and has to use momentum-resolving probes and an energy resolution better than $k_B T^*$. A second problem arises from the surface sensitivity of photoemission techniques, requiring highly ordered single-crystalline surfaces to observe dispersing features. These surfaces can be produced by *in situ* cleaving of layered compounds [6,9–13] or by an *in situ* preparation of thin films of a Ce alloy at the sample surface [14–17]. The second method has the advantage that the surface quality does not depend on the cleave and the quasi-two-dimensional model systems are comparable to theoretical calculations done considering the system structure and dimensionality. It is known that the deposition of 4 ML of Ce and subsequent annealing form a surface alloy that has the same crystal structure as bulk $CePt_5$, as found by combined studies of scanning tunneling microscopy, low-energy electron diffraction (LEED) [18–21], and in the reference compound $LaPt_5$ [22]. This alloy consists of alternating $CePt_2$ and Pt-kagome layers, whereas the topmost layer is a Pt layer which makes the alloy less sensitive to surface oxidation. Thus this system is an ideal model system for studying the effects of the periodic Anderson lattice by angle-resolved photoemission spectroscopy (ARPES). Several earlier investigations on $CePt_5$/Pt(111) surface alloys by photoemission revealed the well-known signature of the Kondo resonance at the Fermi level and even its spin-orbit partner at $E_B \approx 250$ meV [16,17,23,24]. Nevertheless, those experiments were carried out at either too high temperatures or limited by instrumental resolution.

In this Letter we present high-resolution ARPES measurements and dynamical mean-field theory (DMFT) calculations on the $CePt_5$/Pt(111) system. We extract the $4f$ spectral weight as a function of the temperature and show for the first time the transition from a high-temperature phase, in which the system can be described as a set of isolated impurities, to a low-temperature phase where coherent heavy-fermion quasiparticles become apparent. The high-resolution ARPES experiments were performed using a Gammadata R4000 analyzer equipped with a monochromatized discharge lamp using the He II_α emission line ($h\nu = 40.8$ eV, mainly s polarized). The instrumental resolution was determined by measuring the superconducting gap of a V_3Si polycrystal [25], resulting in $\Delta E = 4.3$ meV at the used spectrometer settings. The resonant photoemission experiments were carried out at BL1 of the HiSOR synchrotron radiation source in Hiroshima,

using an SES200 analyzer and linearly polarized light. The total energy resolution (monochromator and analyzer) was $\Delta E = 30$ meV at $h\nu = 122$ eV. Following the method of Ref. [19] we prepared ordered surface alloys by depositing ≈ 4 ML of Ce on a Pt(111) surface. The sample was annealed subsequently for 10 min at ≈ 800 K. The formation of the $CePt_5$ surface alloy was evidenced by LEED experiments (not shown) giving a $(2 \times 2)R30°$ reconstruction, corresponding to a surface alloy with a bulk like $CePt_5$ stoichiometry and geometry [19].

To clarify the electronic structure of the $CePt_5$ surface alloy, Fig. 1 displays measurements at the $4d - 4f$ resonant excitation energy ($h\nu = 122$ eV) at $T = 64$ K, measured in the second Brillouin zone around $\bar{\Gamma}'$. The bottom right panel gives the comparison of the spectrum at the $\bar{\Gamma}'$ point with the off-resonance data ($h\nu = 114$ eV). It shows clearly the main $4f$ features, namely, the KR near the Fermi level E_F, the 7/2 spin-orbit partner (SO) around 0.25 eV, and the ionization peak (IS) at even higher binding energies. The KR, with its maximum a few meV above E_F, reflects the low-energy excitations of the system and shows a distinct temperature dependence [5]. ARPES data at the

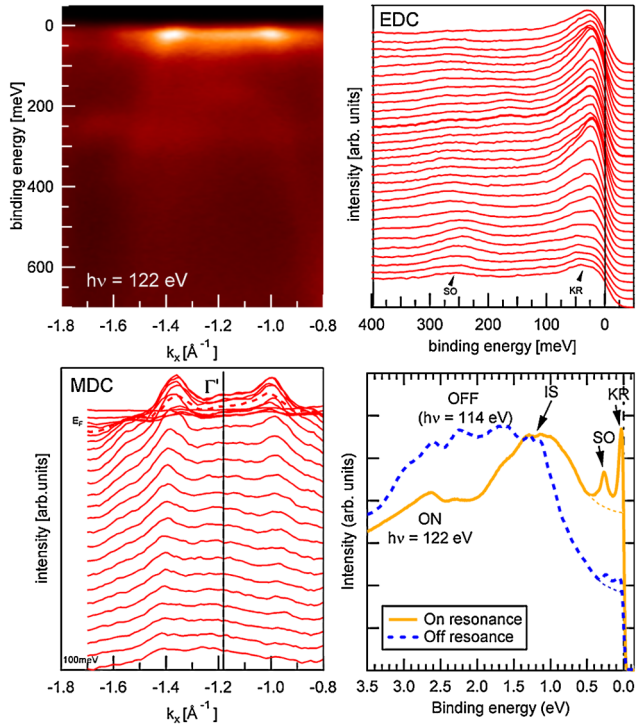

FIG. 1 (color online). Top left: ARPES data set ($\Delta E = 16$ meV, $T = 64$ K) around the $\bar{\Gamma}'$ point (second Brillouin zone) at the $4d$–$4f$ resonance ($h\nu = 122$ eV =). Top right: Energy distribution curves (EDC) taken from top left panel; bottom left: respective momentum distribution curves (MDC) ($\bar{\Gamma}'$ point indicated by thicker line). The data taken at the Fermi level are indicated by a thick dashed line. Bottom right: comparison between the EDC at the $\bar{\Gamma}'$ point measured on- (solid yellow line) and off-resonance (dashed blue line). KR, SO, and IS indicate the Kondo resonance, the spin-orbit partner, and the ionization structure.

resonance energy (other panels) show again these two $4f$ structures, without being able to resolve a band dispersion [see energy distribution curves (EDC, top right panel)], superimposed by the steep conduction band dispersion, which can be found equivalently in the reference compound $LaPt_5$ (not shown). The conduction band appears more clearly in the momentum distribution curves (MDC, bottom left), that represent horizontal cuts through the color-scaled data set at the top. In the following we analyze the high-resolution ARPES data in more detail. Applying a well-established method to restore the thermally occupied part of the spectrum up to an energy of $\approx 5k_BT$ above the Fermi level [26,27] we divide the ARPES spectra recorded along the $\bar{\Gamma}\bar{M}$ direction by the Fermi-Dirac function calculated at the experimental temperature.

Figure 2 shows the resulting data for $T = 13$ K, 34 K, and 66 K. The irregular black or white pattern above the Fermi level is due to the amplified scatter in the experimental background. At the lowest temperature ($T = 13$ K) the intensity maximum is situated right at or slightly above the Fermi level. A few meV below E_F the conduction band sharply bends towards the $\bar{\Gamma}$ point. Additionally, another very narrow horizontal band, pinned at the E_F, appears at larger $|k|$ values. This structure seems to be separated from the conduction band around $\bar{\Gamma}$, as a gapping of the intensity at $|k| = 0.25$ Å^{-1} suggests. The results are consistent with the generic mean-field heavy-fermion picture of a flat f-character band hybridizing with the conduction band of the system. This scenario is sketched in inset to the low-temperature data. To estimate the hybridization gap we plot in Fig. 3 the integrated intensities taken from two momentum regions: $|k| > 0.25$ Å^{-1} and $|k| < 0.1$ Å^{-1}, respectively (as indicated by the nonhatched area in Fig. 2). The region, where the intense conduction band lies, is not taken into account by the integration. The result of the integration is given in Fig. 3: it shows that the binding energies of the intensity maxima differ by $\Delta E_B = 2$ meV. This shift in energy represents a measure for the size of the hybridization gap due to the $d - f$ hybridization between the conduction band and the Ce $4f$ states.

It might be noticed that the experimental data shift towards the unoccupied states with increasing temperature while the maxima in the theoretical spectra stay constantly at E_F. This finding is due to scattering effects in the photoemission process (both from imperfections and from final state effects). Those lead to contributions from other regions in k space, resembling the integrated density of $4f$ states which shows the observed temperature dependent shift [28]. When our calculated spectral function is integrated over the whole Brillouin zone, the maximum shifts towards the unoccupied states as anticipated [5] (inset of Fig. 3). Since this additional contribution is not angle dependent, it does not significantly alter the analysis of the band dispersion.

The hallmark of the heavy-fermion state lies in its temperature dependence. As the temperature is raised,

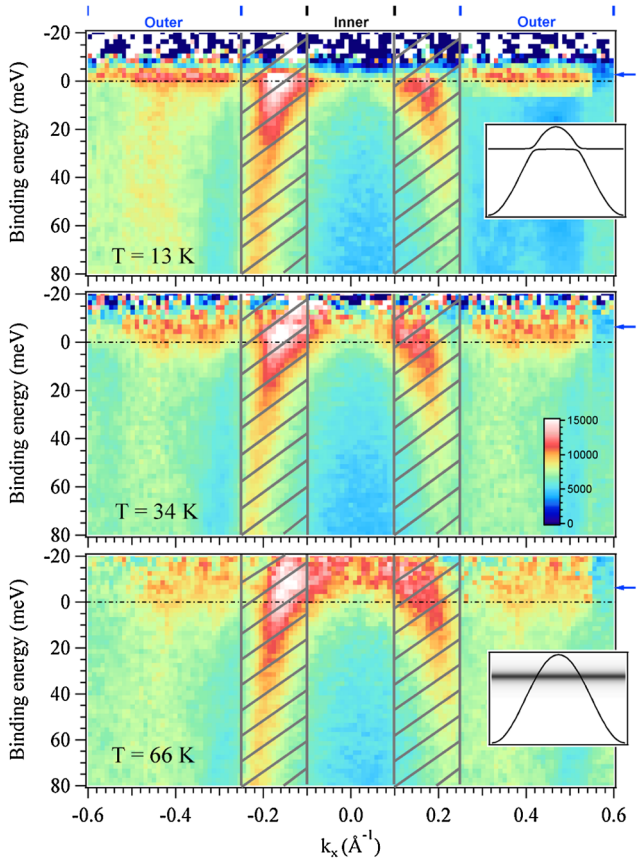

FIG. 2 (color online). Temperature dependence of the ARPES data normalized by the Fermi distribution. The data were acquired as a function of temperature from the lowest to the highest (top to bottom: 13, 34, and 66 K). The spectra show a conduction band (hatched area) and a narrow structure above E_F (indicated by the blue horizontal arrow), the Kondo resonance. With rising temperature, the Kondo resonance broadens and shifts away from E_F. The two insets schematically show the transition from the coherent low-temperature regime to the local regime at high temperatures.

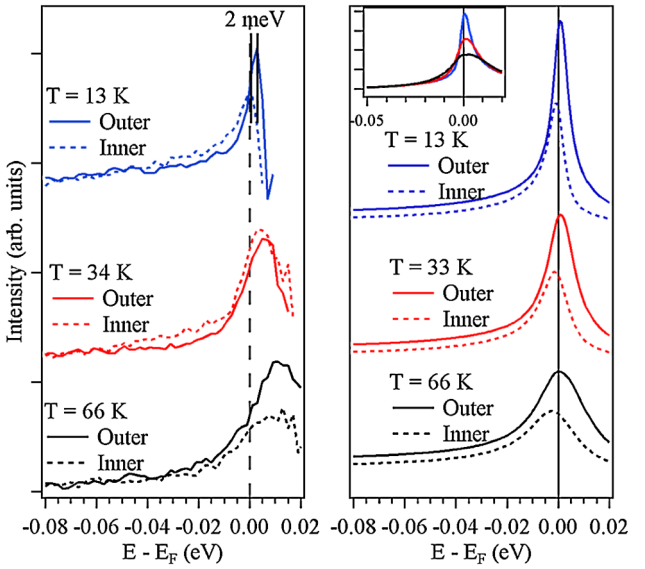

FIG. 3 (color online). Left: integration of the intensity for $|k| > 0.25$ Å^{-1} (solid line) and for $|k| < 0.1$ Å^{-1} (dashed) at three different temperatures. The figure shows that at $T = 13$ K the binding energy of the intensity maxima of the outer- and outer-hybridized bands differ by $\Delta E_B \approx 2$ meV. With rising temperature the difference ΔE_B vanishes. Right: similar quantity as obtained from the modeling of the experiment (see text). In the inset the spectral function integrated over the whole Brillouin zone is shown. The units of the inset x scale are electronvolts.

the hybridized band structure gives way to the bare conduction band thus signaling the crossover from the heavy-fermion state with large Luttinger volume to the high-temperature phase where the f electrons are localized and drop out of the Luttinger volume. The two extreme situations are shown in the insets of Fig. 2. The temperature dependence of the experimental results is consistent with this interpretation. The flat band at $|k| > 0.25$ Å^{-1} broadens and shifts away from E_F. As mentioned above, this temperature dependence is similar to the evolution of the Kondo resonance of systems in which the Ce atoms behave as isolated impurities [5,7]. At the same time the structure around the $\bar{\Gamma}$ point ($|k| < 0.1$ Å^{-1}) acquires spectral weight and evolves towards the emergence of a light band crossing the Fermi energy. This growth in spectral weight is consistent with the closing of the hybridization gap. In the high-temperature limit, i.e., clearly above T_K, and as sketched in the inset, only the conduction band disperses (as sketched in the inset). We note that the temperature dependence is consistent with DMFT calculations for the two-dimensional Kondo lattice [29,30]. The starting point for the theoretical modeling of the experiment presented in Fig. 4 is a tight binding fit of the low-energy features of the bulk reference compound $LaPt_5$. The step to $CePt_5$ is taken at the model level by including an f multiplet. The center position of the f multiplet can be read from Fig. 1 and is set to $\epsilon_f = -1.2$ eV. We have included a spin-orbit splitting of 300 meV and set the Coulomb repulsion to infinity such as to allow solely for $4f^0$ and $4f^1$ configurations. Assuming a k-independent constant hybridization matrix element leaves us with a single free parameter which we set by fitting at best the temperature dependence of the experimental data (see Fig. 3). We solve this multiband Anderson model within the DMFT approximation using a noncrossing approximation (NCA) solver. The details of the approach will be presented elsewhere [31]. Figure 4(a) shows the total spectral function at low temperature, $T = 13$ K. The sharp intense features correspond to the $LaPt_5$ bands. At this low temperature and on this large energy scale we observe distinct rather dispersionless features which stem from the f electrons: (i) the bare f level at $E - E_f \approx -1.2$ eV, (ii) the weak spin-orbit partner of the KR at $E - E_f \approx \pm 0.25$ eV, and (iii) the KR at $E - E_f \approx 0$. The temperature evolution of the spectral function, as given in Figs. 4(c)–4(e) vs energy and momentum, describes nicely

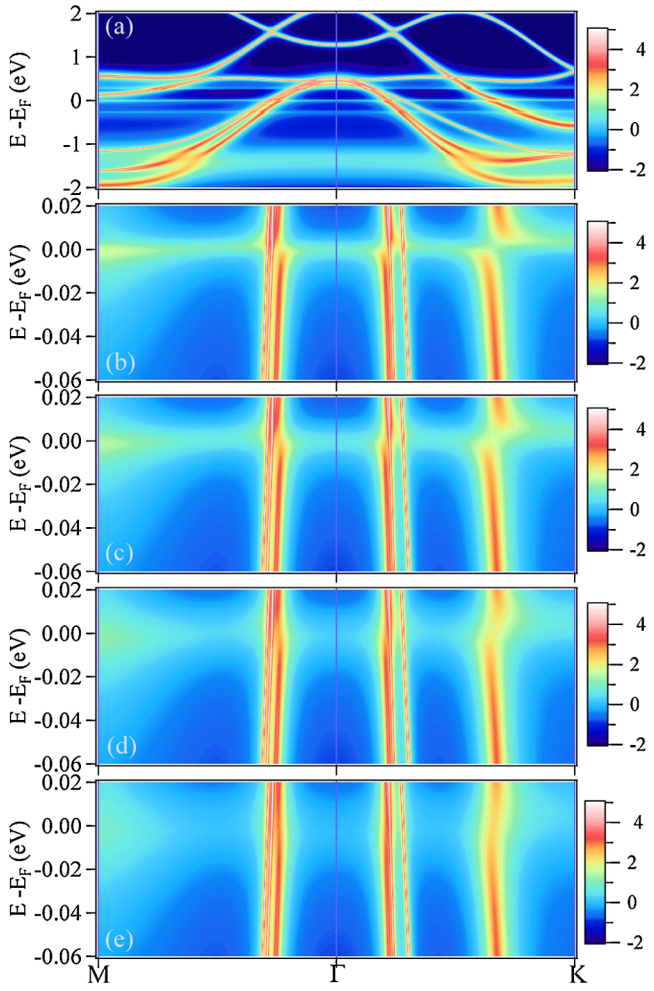

FIG. 4 (color online). (a) Theoretical total spectral function plotted at $T = 13$ K vs energy and momentum in a wide energy scale. Zoom near the Fermi level with (b) $T = 13$ K, (c) $T = 33$ K, (d) $T = 66$ K, (e) $T = 116$ K. In all the panels the intensities are plotted in a logarithmic scale indicated in the bars on the right side of each image. As indicated, the x axis spans k vectors in the first Brillouin zone from the high symmetry point $\bar{M}$ over $\bar{\Gamma}$ to $\bar{K}$.

the experimental findings (see Fig. 2). In the considered temperature range, the emergence of a hybridized band structure, that shows the change of the heavy quasiparticle dispersion and—consequently—the change of the Fermi surface topology, is apparent in this multiband periodic Anderson model.

In conclusion, we demonstrated that on high quality $CePt_5$ films grown on Pt(111), high-resolution ARPES experiments allow us to extract the temperature dependence of the $4f$ spectral weight. At high temperatures we observe the well-known Kondo resonance with a less intense spin-orbit feature, superimposed by the conduction bands. At low temperatures a remarkable change in the band dispersion appears: in the vicinity of the Fermi level the Kondo resonance evolves into hybridized heavy quasiparticle bands thus signaling, at the single-particle level, the onset of the coherent heavy-fermion Fermi-liquid state. A comparison with DMFT + NCA calculations of a multiband Anderson model which takes into account the band structure of the reference compound, $LaPt_5$, supports these conclusions and allows a detailed analysis of the microscopic interactions.

This work was supported by the JSPS and the Deutsche Forschungsgemeinschaft within the Forschergruppe 1162. We would like to thank Hans Kroha for helpful discussions. The synchrotron-radiation experiments were done under the approval of HSRC Proposal No. 07-A-42. We acknowledge the FOR1162 DFG project for financial support.

*Corresponding author.
reinert@physik.uni-wuerzburg.de

[1] H. v. Löhneysen *et al.*, Rev. Mod. Phys. **79**, 1015 (2007).
[2] A. C. Hewson, *The Kondo Problem to Heavy Fermions* (Cambridge University Press, Cambridge, U.K., 1993).
[3] O. Gunnarsson and K. Schönhammer, Phys. Rev. Lett. **50**, 604 (1983).
[4] O. Gunnarsson and K. Schönhammer, Phys. Rev. B **28**, 4315 (1983).
[5] N. E. Bickers, D. L. Cox, and J. W. Wilkins, Phys. Rev. B **36**, 2036 (1987).
[6] J. W. Allen, J. Phys. Soc. Jpn. **74**, 34 (2005).
[7] D. Ehm *et al.*, Phys. Rev. B **76**, 045117 (2007).
[8] P. Fulde, *Electron Correlations in Molecules and Solids* (Springer-Verlag, Berlin, Heidelberg, New York, 1993).
[9] J. D. Denlinger *et al.*, J. Electron Spectrosc. Relat. Phenom. **117–118**, 347 (2001).
[10] G. A. Wigger *et al.*, Phys. Rev. B **76**, 035106 (2007).
[11] D. V. Vyalikh *et al.*, Phys. Rev. Lett. **100**, 056402 (2008).
[12] H. J. Im *et al.*, Phys. Rev. Lett. **100**, 176402 (2008).
[13] A. Koitzsch *et al.*, Phys. Rev. B **77**, 155128 (2008).
[14] M. Garnier *et al.*, Phys. Rev. B **56**, R11399 (1997).
[15] S. Danzenbächer *et al.*, Phys. Rev. B **72**, 033104 (2005).
[16] M. Garnier *et al.*, Phys. Rev. B **58**, 9697 (1998).
[17] T. Pillo *et al.*, Physica (Amsterdam) **259B–261B**, 1118 (1999).
[18] J. Tang, J. M. Lawrence, and J. C. Hemminger, Phys. Rev. B **48**, 15 342 (1993).
[19] C. J. Baddeley *et al.*, Phys. Rev. B **56**, 12 589 (1997).
[20] U. Berner and K. D. Schierbaum, Phys. Rev. B **65**, 235404 (2002).
[21] B. Vermang, M. Juel, and S. Raaen, Phys. Rev. B **73**, 033407 (2006).
[22] A. Ramstad and S. Raaen, Phys. Rev. B **59**, 15 935 (1999).
[23] A. B. Andrews *et al.*, Phys. Rev. B **51**, 3277 (1995).
[24] M. Garnier *et al.*, Phys. Rev. Lett. **78**, 4127 (1997).
[25] F. Reinert *et al.*, Phys. Rev. Lett. **85**, 3930 (2000).
[26] T. Greber, T. J. Kreutz, and J. Osterwalder, Phys. Rev. Lett. **79**, 4465 (1997).
[27] F. Reinert *et al.*, Phys. Rev. Lett. **87**, 106401 (2001).
[28] D. Ehm *et al.*, Phys. Rev. B **64**, 235104 (2001).
[29] K. S. D. Beach and F. F. Assaad, Phys. Rev. B **77**, 205123 (2008).
[30] See supplemental material at http://link.aps.org/supplemental/10.1103/PhysRevLett.106.186407 for a model calculation of a simple two-band model.
[31] F. F. Assaad and J. Werner (unpublished).